SUPPORTING INFORMATION

The Bacterial Ammonia Lyase EncP: A Tunable Biocatalyst for the Synthesis of Unnatural Amino Acids

Nicholas J. Weise, Fabio Parmeggiani, Syed T. Ahmed and Nicholas J. Turner*

Table of contents **Page**

* corresponding author (e-mail nicholas.turner@manchester.ac.uk)

Additional figures of the homology model of EncP

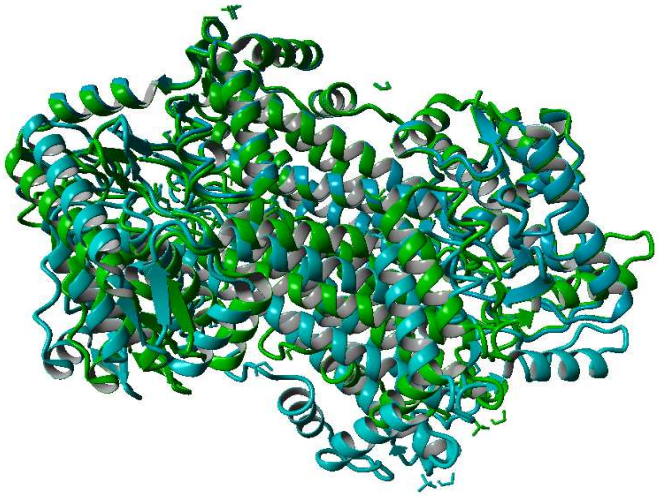

Figure S1. Comparison of the 3D structure of AdmH (green) with the homology model built for EncP (cyan).

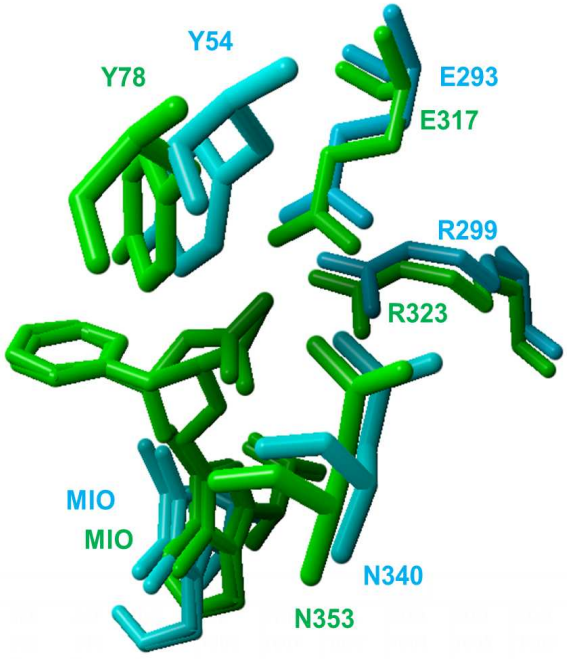

Figure S2. Comparison of the active site residues of AdmH (green) with the homology model built for EncP (cyan). The structure of AdmH also shows (*S*)-**2a** and (*S*)-**3a** bound to the MIO cofactor.

Purification of EncP and SDS-PAGE analysis

E. coli BL21(DE3) whole cells containing the PAL variant (1.5 g wet weight) were resuspended in wash buffer (15 mL, 50 mM KP_i, 300 mM NaCl, 20 mM imidazole, pH 7.4). Lysozyme (1 mg mL^{-1}) was added and the mixture was incubated at 37°C and 220 rpm for 45 min. The suspension was sonicated (12 μm amplitude, 20 s on, 20 s off, 10 cycles, Soniprep 150, MSE UK Ltd.) on ice and treated with DNAse (100 μL, 1 mg mL^{-1}) at 37°C and 220 rpm for 30 min. The mixture was centrifuged (18000 rpm, 20 min, 4°C) and the supernatant was filtered (0.45 μm and 0.2 μm syringe filters) and loaded onto a pre-packed HisTrap FF column (GE Healthcare, 5 mL solid phase). The column was washed with the same wash buffer (25-50 mL) and with a 20:1 mixture (50 mL) of wash buffer and elution buffer (50 mM KP_i, 500 mM NaCl, 500 mM imidazole, pH 7.4). The protein was eluted with elution buffer (50 mL), collecting the eluate in different fractions. Fractions were pooled according to the protein concentration (measured by Bradford assay) and purity (judged by SDS-PAGE analysis). The pooled fractions were concentrated and desalted by buffer exchange in a disposable centrifugal filter (100 kDa MWCO, Sartorius Stedim).

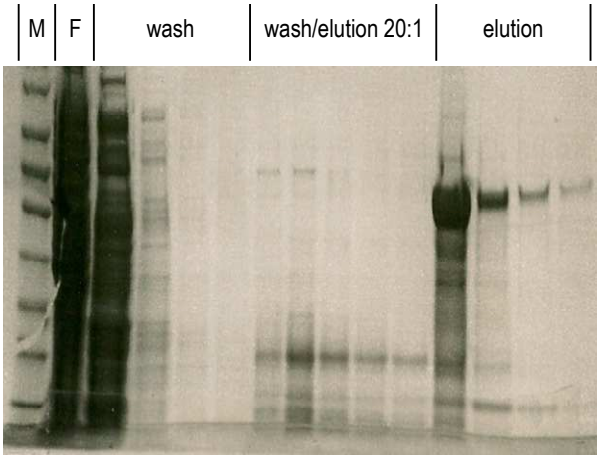

Figure S3. SDS-PAGE analysis of selected fractions from the purification of EncP produced with autoinduction media (M: molecular weight marker, F: flow-through).

Optimization of EncP-WT biotransformations

Table S1. The effect of ammonium donor salt on the conversion of cinnamate **1a** and β:α ratio of products in EncP-catalysed biotransformations (70°C, 22 h).

Ammonium donor salt	Conv. (%)	β:α ratio
ammonium acetate, 1 M, pH 8.6	23	62:38
ammonium chloride, 1 M, pH 8.5	25	53:47
ammonium nitrate, 1 M, pH 8.4	23	49:51
ammonium sulfate, 1 M, pH 8.6	34	55:45

Table S2. The effect of ammonium sulfate concentration on the conversion of cinnamate **1a** in EncP biotransformations (pH 8.3, 70°C, 22 h).

Conc.		0.5 M	1.0 M	1.5 M	2.0 M	3.0 M	4.0 M
Conv. (%)	repl. 1	15	23	35	47	64	73
	repl. 2	15	23	38	46	65	75
	repl. 3	16	25	34	44	65	73
	mean	**15**	**24**	**35**	**46**	**64**	**74**

Table S3. The effect of buffer pH on the conversion of cinnamate **1a** in EncP biotransformations (4 M ammonium sulfate, 70°C, 22 h).

pH		7.0	8.0	9.0	10.0
Conv. (%)	repl. 1	50	60	60	62
	repl. 2	45	61	58	60
	repl. 3	45	62	62	63
	mean	**46**	**61**	**60**	**62**

Table S4. The effect of incubation temperature on the conversion of cinnamate **1a** and β:α ratio of products in EncP-catalysed biotransformations (4 M ammonium sulfate, pH 8.3, 22 h).

Temperature	Conv. (%)	β:α ratio
25°C	22	52:48
40°C	52	57:43
55°C	83	58:42
70°C	74	58:42
85°C	24	75:25

Further details on the rational design of EncP variants

Residue R323 in AdmH forms a monodentate salt bridge with the substrate and is the main interaction of the carboxyl binding pocket with the bound ligand. This arginine is completely conserved across all class I lyase-like sequences, indicating the importance of this salt bridge across the enzyme family for binding of various aromatic amino acids and arylacrylates. For this reason an arginine to lysine mutation was considered for the homologous position in EncP (R299) so as to maintain this interaction. There are reports in the literature of two active mutations made at this position in a histidine ammonia-lyase (PpHAL from *Pseudomonas putida*). The R283I mutations decreased enzyme activity by 1640-fold whereas the R283K variant enzyme was only 20 times less active than the wild-type.[S1] These results reinforced the choice of mutation, as it was likely that the EncP R299K variant would be active.

Biotransformations run with cinnamate and EncP-R299K-containing whole cells showed an increase in β-selective amination compared to with the wild-type enzyme. Interestingly the β-:α-product ratio was found to be temperature dependent, with an excess of between 2-3 fold β-phenylalanine product observed at 25°C, 40°C and 70°C. At 55°C, however, the ratio was over 9:1. The temperature profile of the whole cell reaction was also found to be altered with respect to the wild-type. The temperature optimum of the new variant was estimated to be ~45°C, around 20°C lower than the wild-type (Figure S4). This may be due to the deformation of the carboxyl binding pocket by the substitution of arginine by an amino acid of different shape, decreasing the stability of the active site at higher temperatures. This is in line with the reported lowered activity of the PpHAL R283K variant[S1] and hypotheses of a delicate hydrogen bonding network around the carboxyl binding pocket in related PAL enzymes.[S2]

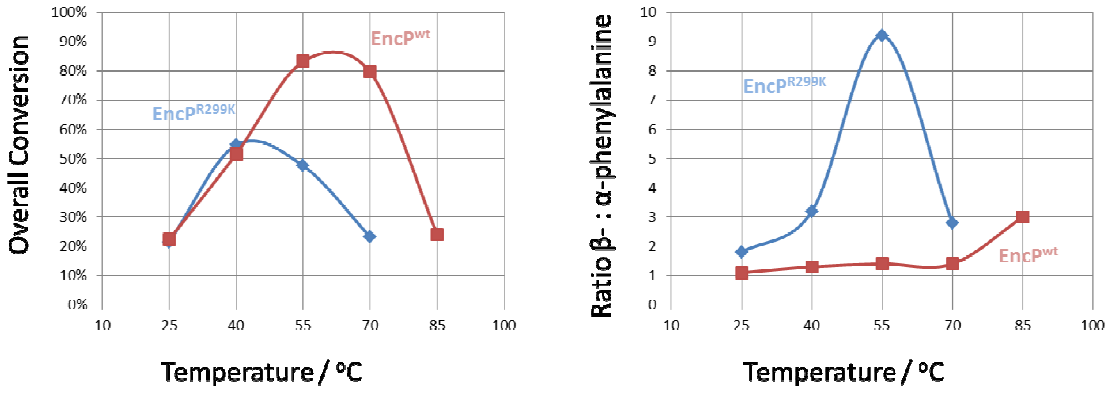

Figure S4. Influence of temperature on overall conversion (left) and β-:α-product ratio (right) in amination reactions of **1a** catalysed by wild-type EncP and the R299K variant.

The temperature profile of the E293Q variant is curious in that this time the optimum is estimated to be ~15°C higher than the wild-type (Figure S5). The conservation of Q at this position in other enzymes could be hypothesised as being important for stability of the delicate active site. It also

provides evidence for an interesting theory that a common ancestor of EncP and AdmH experienced a Q to E substitution to the detriment of protein stability but enhancing β-regioselectivity and, most likely, aminomutase activity.

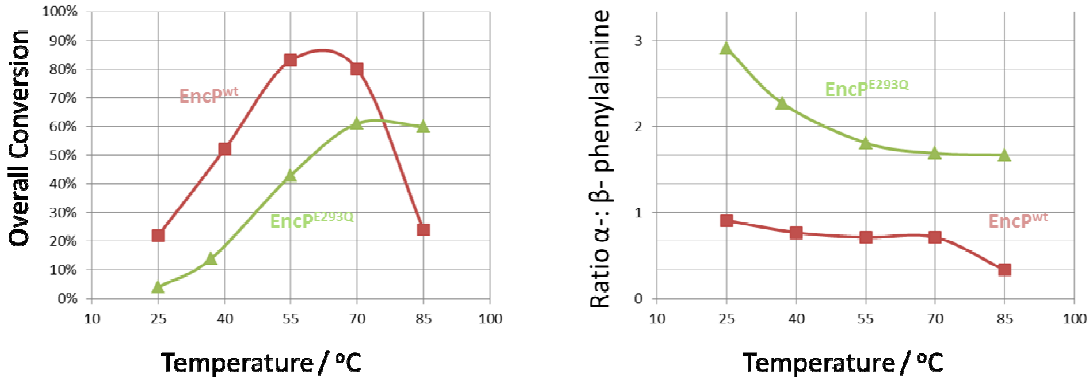

Figure S5. Influence of temperature on overall conversion (left) and α-:β-product ratio (right) in amination reactions of **1a** catalysed by wild-type EncP and the E293Q variant.

Concerning variant E293M, again the addition preference was temperature-dependent but even the least α-selective biotransformations produced ~4 times as much α-phenylalanine as β- (Figure S6). The odd overall conversion profile shows that the enzyme turnover varies a lot less with temperature compared with the other variants, implying that the E293M mutation may also be detrimental to the stability of the enzyme active site. This could explain why only Q and E are seen in this position in nature; they are the best amino acids to retain an optimal active site shape for catalysis under physiological conditions.

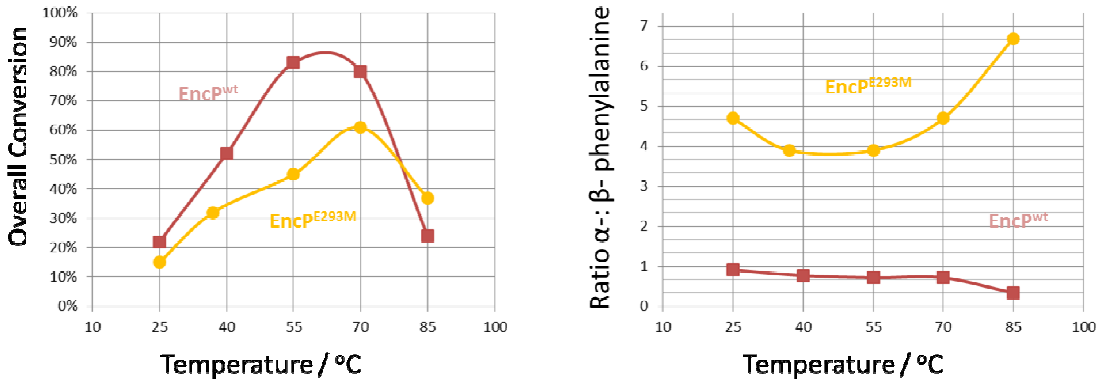

Figure S6. Influence of temperature on overall conversion (left) and α-:β-product ratio (right) in amination reactions of **1a** catalysed by wild-type EncP and the E293M variant.

Complete data set for the amination of arylacrylic acids 1a-v

Figure S7 provided below is an expanded version of Figure 3 (from the main text), including also the results of the biotransformations with the variant E293Q. The complete data set used to generate these figures is provided in Tables S5-S8.

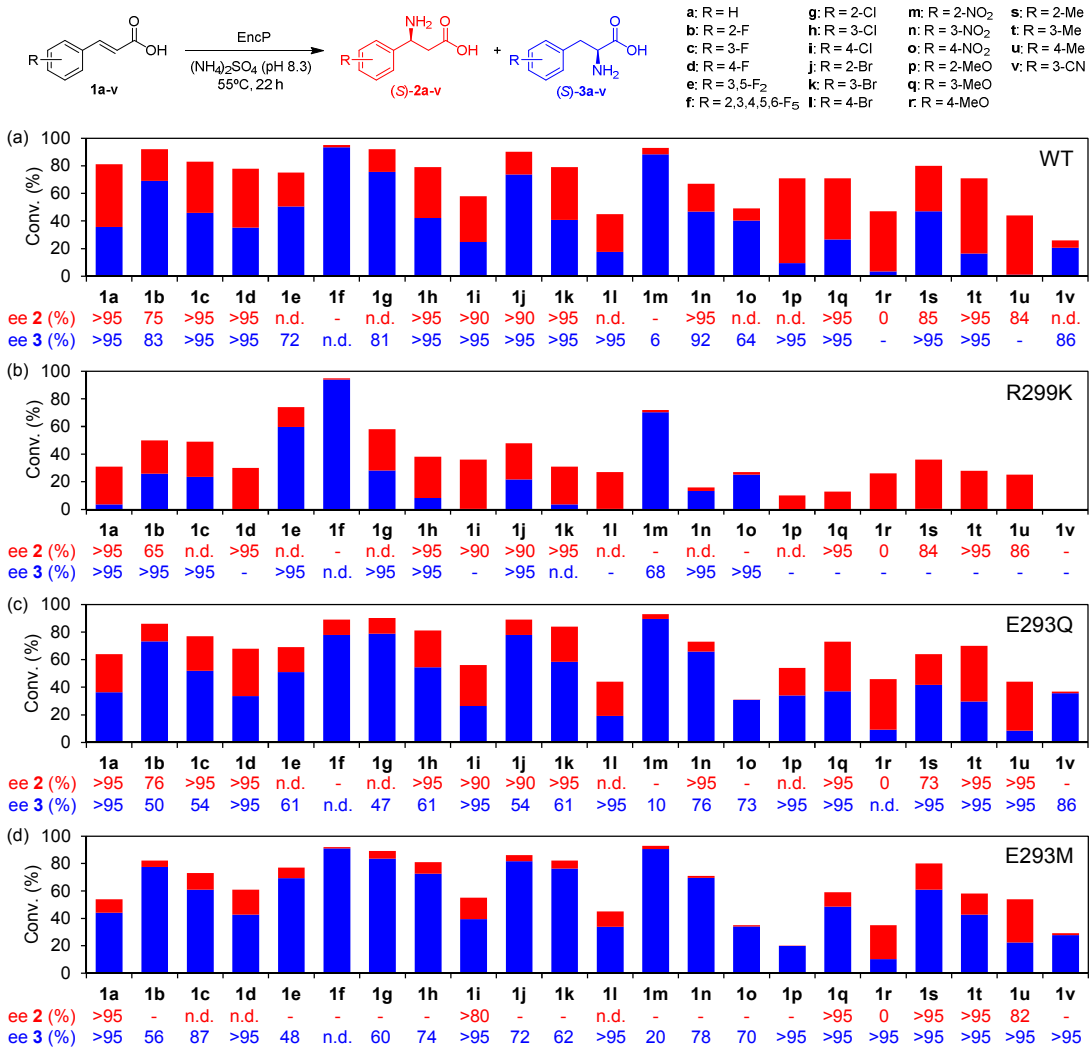

Figure S7. Amination of arylacrylic acids **1a-v** to the corresponding amino acids by EncP and three rationally designed regioselective variants.

Table S5. Amination of arylacrylic acids **1a-v** by the EncP wild-type enzyme.

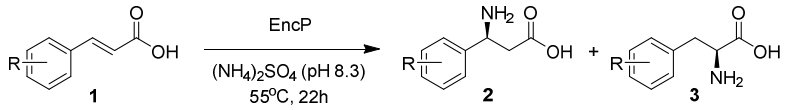

1	R	Conv. (2:3)[a]	ee of 2[b]	ee of 3[b]
1a	H	81% (56:44)	>95% *(S)*	>95% *(S)*
1b	2-F	92% (25:75)	75% *(S)*	83% *(S)*
1c	3-F	83% (45:55)	>95% *(S)*	>95% *(S)*
1d	4-F	78% (55:45)	>95% *(S)*	>95% *(S)*
1e	3,5-F_2	75% (33:67)	n.d.	72% *(S)*
1f	2,3,4,5,6-F_5	95% (2:98)	–	n.d.
1g	2-Cl	92% (18:82)	n.d.	81% *(S)*
1h	3-Cl	79% (47:53)	>95% *(S)*	>95% *(S)*
1i	4-Cl	58% (57:43)	>90% *(S)*	>95% *(S)*
1j	2-Br	90% (18:82)	>90% *(S)*	>95% *(S)*
1k	3-Br	79% (48:52)	>95% *(S)*	>95% *(S)*
1l	4-Br	45% (61:39)	n.d.	>95% *(S)*
1m	2-NO_2	93% (5:95)	–	6% *(S)*
1n	3-NO_2	67% (30:70)	>95% *(S)*	92% *(S)*
1o	4-NO_2	49% (18:82)	n.d.	64% *(S)*
1p	2-MeO	71% (87:13)	n.d.	>95% *(S)*
1q	3-MeO	71% (62:38)	>95% *(S)*	>95% *(S)*
1r	4-MeO	47% (93:7)	0	–
1s	2-Me	80% (41:59)	85% *(S)*	>95% *(S)*
1t	3-Me	71% (77:23)	>95% *(S)*	>95% *(S)*
1u	4-Me	44% (97:3)	84% *(S)*	–
1v	3-CN	26% (21:79)	n.d.	86% *(S)*

n.d. = not determined; – = not required; [a] conversions and product ratios determined by non-chiral HPLC; [b] enantiomeric excesses determined by chiral HPLC.

Table S6. Amination of arylacrylic acids **1a-v** by the EncP-R299K rationally designed variant.

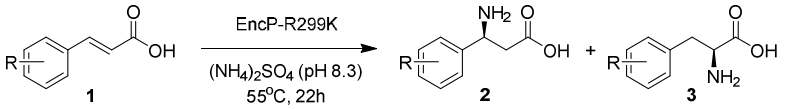

1	R	Conv. (2:3)[a]	ee of 2[b]	ee of 3[b]
1a	H	31% (88:12)	>95% *(S)*	>95% *(S)*
1b	2-F	50% (48:53)	65% *(S)*	>95% *(S)*
1c	3-F	49% (52:48)	n.d.	>95% *(S)*
1d	4-F	30% (99:1)	>95% *(S)*	–
1e	3,5-F_2	74% (19:81)	n.d.	>95% *(S)*
1f	2,3,4,5,6-F_5	95% (1:99)	–	n.d.
1g	2-Cl	58% (51:49)	n.d.	>95% *(S)*
1h	3-Cl	38% (78:22)	>95% *(S)*	>95% *(S)*
1i	4-Cl	36% (99:1)	>90% *(S)*	–
1j	2-Br	48% (55:45)	>90% *(S)*	>95% *(S)*
1k	3-Br	31% (88:12)	>95% *(S)*	n.d.
1l	4-Br	27% (99:1)	n.d.	–
1m	2-NO_2	72% (2:98)	–	68% *(S)*
1n	3-NO_2	16% (17:83)	n.d.	>95% *(S)*
1o	4-NO_2	27% (7:93)	–	>95% *(S)*
1p	2-MeO	10% (99:1)	n.d.	–
1q	3-MeO	13% (99:1)	>95% *(S)*	–
1r	4-MeO	26% (99:1)	0	–
1s	2-Me	36% (99:1)	84% *(S)*	–
1t	3-Me	28% (99:1)	>95% *(S)*	–
1u	4-Me	25% (99:1)	86% *(S)*	–
1v	3-CN	<1% (–:–)	–	–

n.d. = not determined; – = not required; [a] conversions and product ratios determined by non-chiral HPLC; [b] enantiomeric excesses determined by chiral HPLC.

Table S7. Amination of arylacrylic acids **1a-v** by the EncP-E293Q rationally designed variant.

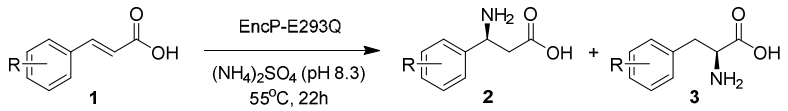

1	R	Conv. (**2**:**3**)[a]	ee of **2**[b]	ee of **3**[b]
1a	H	64% (43:57)	>95% *(S)*	>95% *(S)*
1b	2-F	86% (15:85)	76% *(S)*	50% *(S)*
1c	3-F	77% (32:68)	>98% *(S)*	54% *(S)*
1d	4-F	68% (51:49)	>95% *(S)*	>95% *(S)*
1e	3,5-F_2	69% (26:74)	n.d.	61% *(S)*
1f	2,3,4,5,6-F_5	89% (2:98)	–	n.d.
1g	2-Cl	90% (12:88)	n.d.	47% *(S)*
1h	3-Cl	81% (33:67)	>95% *(S)*	61% *(S)*
1i	4-Cl	56% (53:47)	>90% *(S)*	>95% *(S)*
1j	2-Br	89% (13:87)	>90% *(S)*	54% *(S)*
1k	3-Br	84% (30:70)	>95% *(S)*	61% *(S)*
1l	4-Br	44% (56:44)	n.d.	>95% *(S)*
1m	2-NO_2	93% (4:96)	–	10% *(S)*
1n	3-NO_2	73% (10:90)	>95% *(S)*	76% *(S)*
1o	4-NO_2	31% (1:99)	–	73% *(S)*
1p	2-MeO	54% (37:63)	n.d.	>95% *(S)*
1q	3-MeO	73% (49:51)	>95% *(S)*	>95% *(S)*
1r	4-MeO	46% (80:20)	0	n.d.
1s	2-Me	64% (35:65)	73% *(S)*	>95% *(S)*
1t	3-Me	70% (58:42)	>95% *(S)*	>95% *(S)*
1u	4-Me	44% (80:20)	>95% *(S)*	>95% *(S)*
1v	3-CN	37% (4:96)	–	86% *(S)*

n.d. = not determined; – = not required; [a] conversions and product ratios determined by non-chiral HPLC; [b] enantiomeric excesses determined by chiral HPLC.

Table S8. Amination of arylacrylic acids **1a-v** by the EncP-E293M rationally designed variant.

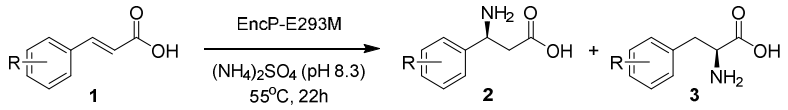

1	R	Conv. (**2**:**3**)[a]	ee of **2**[b]	ee of **3**[b]
1a	H	54% (18:82)	>95% *(S)*	>95% *(S)*
1b	2-F	82% (5:95)	–	56% *(S)*
1c	3-F	73% (16:84)	n.d.	87% *(S)*
1d	4-F	61% (30:70)	n.d.	>95% *(S)*
1e	3,5-F_2	77% (10:90)	–	48% *(S)*
1f	2,3,4,5,6-F_5	92% (1:99)	–	n.d.
1g	2-Cl	92% (6:94)	–	60% *(S)*
1h	3-Cl	81% (10:90)	–	74% *(S)*
1i	4-Cl	55% (28:72)	>80% *(S)*	>95% *(S)*
1j	2-Br	86% (5:95)	–	72% *(S)*
1k	3-Br	82% (7:93)	–	62% *(S)*
1l	4-Br	45% (25:75)	n.d.	>95% *(S)*
1m	2-NO_2	93% (3:97)	–	20% *(S)*
1n	3-NO_2	71% (2:98)	–	78% *(S)*
1o	4-NO_2	35% (3:97)	–	70% *(S)*
1p	2-MeO	20% (1:99)	–	>95% *(S)*
1q	3-MeO	59% (18:82)	>95% *(S)*	>95% *(S)*
1r	4-MeO	35% (71:29)	0	>95% *(S)*
1s	2-Me	80% (24:76)	>95% *(S)*	>95% *(S)*
1t	3-Me	58% (26:74)	>95% *(S)*	>95% *(S)*
1u	4-Me	54% (59:41)	82% *(S)*	>95% *(S)*
1v	3-CN	29% (5:95)	–	>95% *(S)*

n.d. = not determined; – = not required; [a] conversions and product ratios determined by non-chiral HPLC; [b] enantiomeric excesses determined by chiral HPLC.

HPLC analysis

Reverse phase HPLC analyses were performed on an Agilent 1200 Series system equipped with a G1379A degasser, G1312A binary pump, a G1329 autosampler unit, a G1316A temperature controlled column compartment and a G1315B diode array detector. Where appropriate, an external column cooling jacket was employed instead of the temperature controlled column compartment.

Conversion and product distribution analyses were performed on a ZORBAX Extend-C18 column (50 mm × 4.6 mm × 3.5 μm Agilent). Mobile phase: NH_4OH buffer (0.35% w/v, pH 10.0) / MeOH (see Table S9). Flow rate: 1 mL min^{-1}. Temperature: 40°C. Detection wavelength: 210 nm. Retention times are given in Table S9. Peaks were assigned via comparison with commercially available standards. Conversions and product ratios were calculated from peak area integrations with use of appropriate response factors (Table S9).

Fractions (100-200 μL) were collected from these analytical runs for subsequent chiral analysis. Enantiomeric excesses were measured using a Crownpak CR (+) HPLC column, (150 mm × 4 mm × 5 μm, Daicel). Mobile phase: aq. $HClO_4$ (1.14% w/v, pH 2.0) / MeOH (see Table S10). Flow rate: 1 mL min^{-1} for runs at 25°C and 0.5 mL min^{-1} for runs at –8°C. Temperature: see Table S10. Detection wavelength: 210 nm. Retention times are given in Table S10. Peaks were assigned via comparison with the literature[S3] and with commercially available standards. Enantiomeric excess values were calculated from peak area integrations.

Table S9. HPLC conditions and retention times for non-chiral analyses.

Compound		MeOH [%]	Temp. [°C]	Retention time [min]			Response factor (1 vs. 3)
	R			**2**	**3**	**1**	
a	H	10	40	1.8	2.3	5.4	2.3
b	2-F	10	40	2.2	2.8	7.2	2.8
c	3-F	10	40	2.4	3.0	7.7	2.7
d	4-F	10	40	2.3	2.7	7.1	2.8
e	$3,5\text{-}F_2$	20	40	2.1	2.5	6.4	2.9
f	$2,3,4,5,6\text{-}F_5$	30	40	1.7	2.6	6.8	3.2
g	2-Cl	20	40	2.5	3.0	7.4	2.2
h	3-Cl	30	40	1.8	2.2	4.8	2.1
i	4-Cl	30	40	1.9	2.3	5.0	2.0
j	2-Br	30	40	1.8	2.1	4.3	1.4
k	3-Br	30	40	2.2	2.8	6.2	1.5
l	4-Br	30	40	2.3	2.9	6.5	1.4
m	$2\text{-}NO_2$	10	40	2.3	3.9	5.9	1.5
n	$3\text{-}NO_2$	10	40	2.2	3.1	6.8	1.4
o	$4\text{-}NO_2$	10	40	1.8	2.8	6.1	2.1
p	$2\text{-}OCH_3$	20	40	1.7	2.3	4.5	2.0
q	$3\text{-}OCH_3$	20	40	1.5	1.9	4.0	1.9
r	$4\text{-}OCH_3$	10	40	1.7	2.2	6.4	2.1
s	$2\text{-}CH_3$	20	40	2.1	2.8	6.6	2.0
t	$3\text{-}CH_3$	20	40	2.5	3.2	7.7	2.1
u	$4\text{-}CH_3$	20	40	2.4	3.5	7.1	2.0
v	3-CN	10	40	1.8	2.5	5.1	1.2

Table S10. HPLC conditions and retention times for chiral analyses.

Compound		MeOH [%]	Temp. [°C]	Retention time [min]	
	R			(*R*)-enantiomer	(*S*)-enantiomer
2a	H	14	–8	120.6	93.3
3a		4	25	5.0	6.3
2b	2-F	14	–8	43.6	26.7
3b		4	25	5.8	7.5
2c	3-F	4	25	8.8	10.6
3c		4	25	6.5	8.3
2d	4-F	14	–8	82.8	63.9
3d		4	25	6.6	8.1
2e	3,5-F_2	–	–	–	–
3e		4	0	7.4	9.0
2f	2,3,4,5,6-F_5	–	–	–	–
3f		–	–	–	–
2g	2-Cl	–	–	–	–
3g		14	25	8.1	10.1
2h	3-Cl	14	–8	14.7	25.2
3h		14	25	11.1	15.3
2i	4-Cl	14	–8	252.1	214.7
3i		14	25	11.4	14.1
2j	2-Br	14	–8	146.2	131.3
3j		14	25	12.1	15.4
2k	3-Br	14	25	21.3	40.1
3k		14	25	19.7	24.8
2l	4-Br	–	–	–	–
3l		14	25	18.2	23.7
2m	2-NO_2	4	25	6.0	8.8
3m		4	25	6.5	8.1
2n	3-NO_2	4	25	9.0	13.2
3n		4	25	7.4	10.6
2o	4-NO_2	–	–	–	–
3o		4	25	7.7	8.9
2p	2-MeO	–	–	–	–
3p		4	25	11.3	14.1
2q	3-MeO	4	25	13.4	15.5
3q		4	25	13.9	17.1
2r	4-MeO	14	–8	162.1	111.2
3r		14	25	6.8	9.2
2s	2-Me	4	25	14.2	12.0
3s		4	25	11.5	13.7
2t	3-Me	4	25	10.1	12.9
3t		4	25	15.4	18.1
2u	4-Me	4	–8	168.4	143.7
3u		4	25	14.9	18.4
2v	3-CN	–	–	–	–
3v		4	25	5.0	6.4

Chiral HPLC chromatograms of compounds 2a-v and 3a-v

Representative chiral HPLC traces for reference samples of racemic compounds **2a-v** and **3a-v** are provided below. Good separation of almost all pairs of enantiomers has been obtained (baseline in most cases). Traces for compounds **2e**, **2f**, **3f**, **2g**, **2l**, **2o**, **2p**, **2v** are not shown because a satisfactory separation of the two enantiomers could not be achieved with the methods tested (and the corresponding ee values could not be measured). As such, these data points are noted as n.d. (not determined) in Tables S5-S8 and Figure S7.

Racemic samples were obtained from commercial sources with the following exceptions: samples of β-amino acids **2e**, **2k**, **2n**, **2q** and **2s-u** were synthesized as reported in the literature;[S4] samples of α-amino acids **3h**, **3k**, **3n** and **3r-v** (not completely racemic) have been obtained by partial racemization of the commercially available (*S*)-enantiomers, employing the deracemization method described previously.[S5]

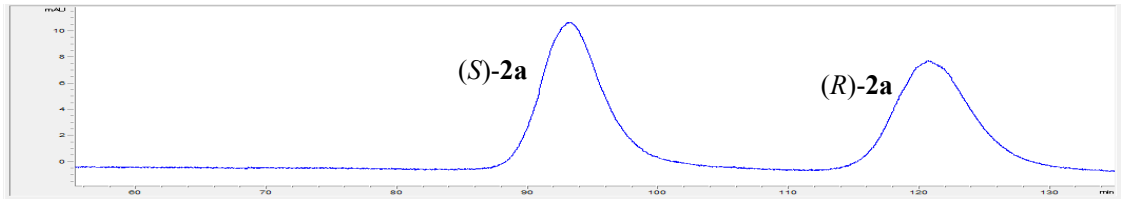

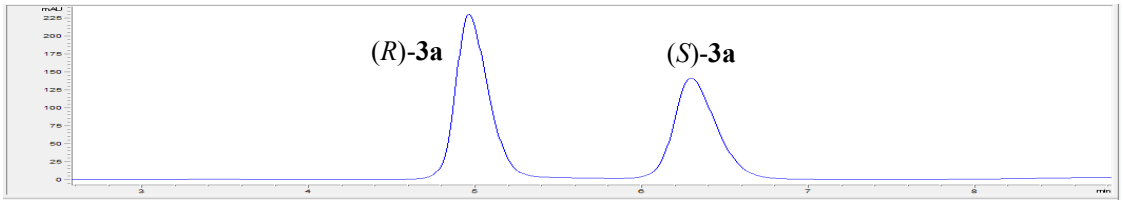

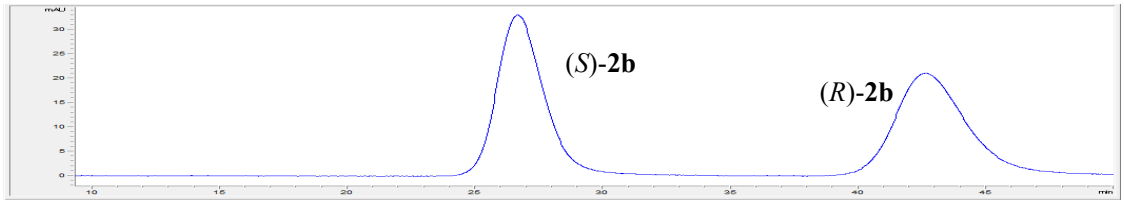

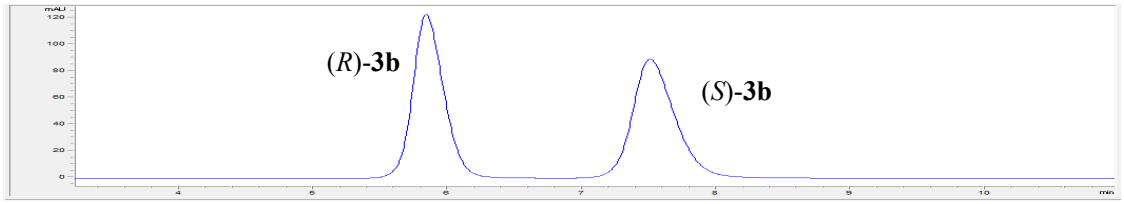

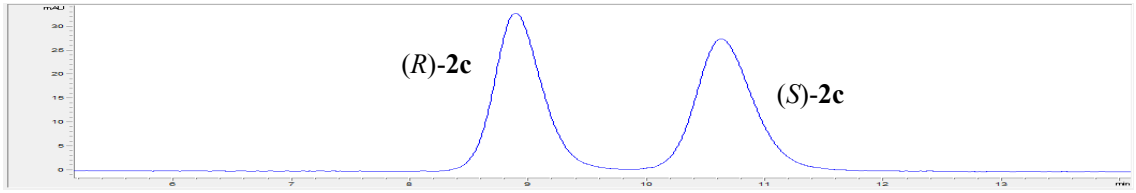
(R)-2c
(S)-2c

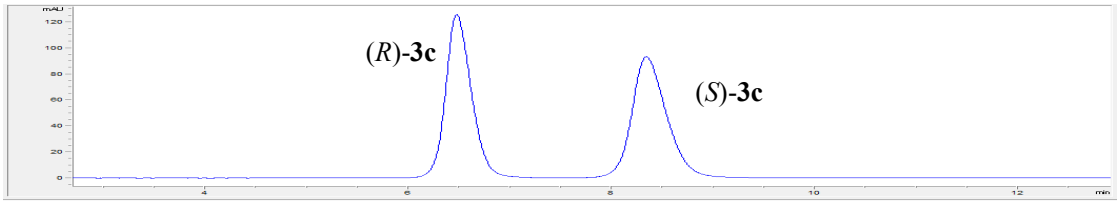
(R)-3c
(S)-3c

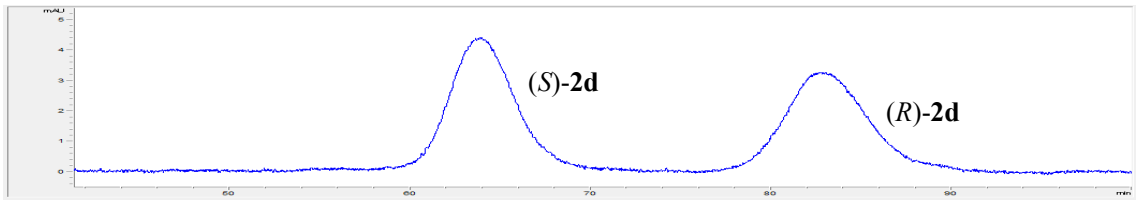
(S)-2d
(R)-2d

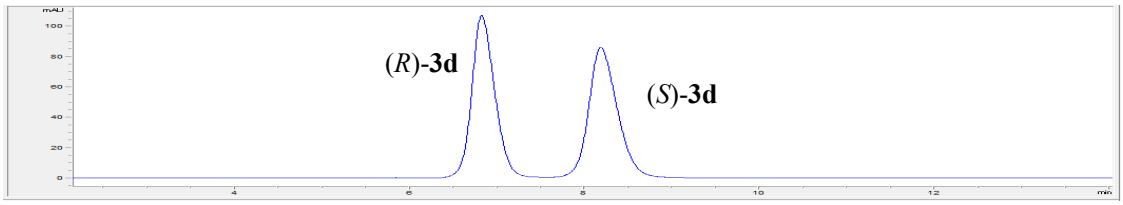
(R)-3d
(S)-3d

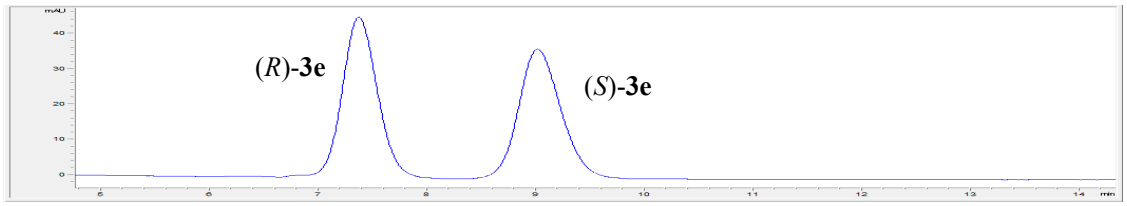
(R)-3e
(S)-3e

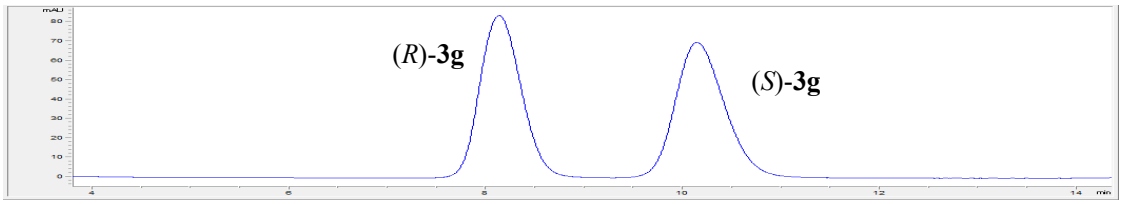
(R)-3g
(S)-3g

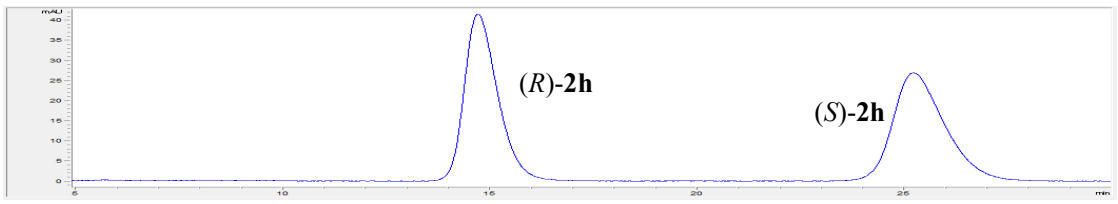
(R)-2h
(S)-2h

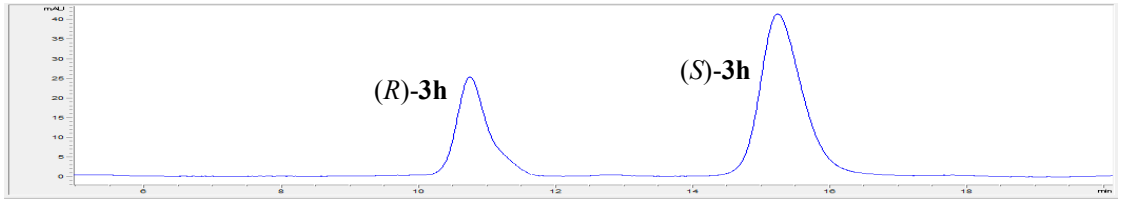
(R)-3h
(S)-3h

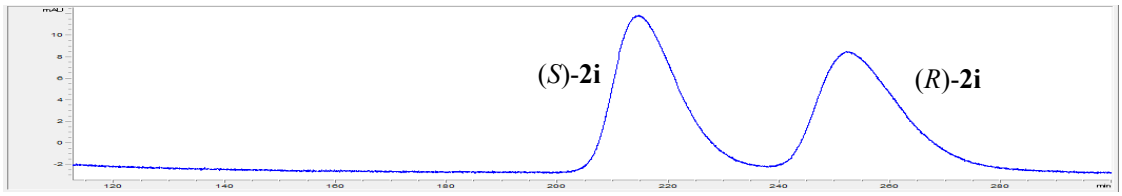
(S)-2i
(R)-2i

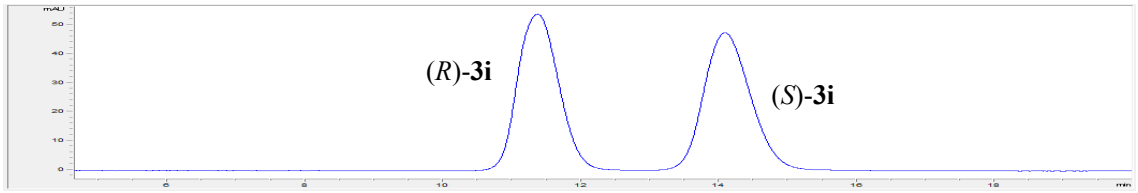
(R)-3i
(S)-3i

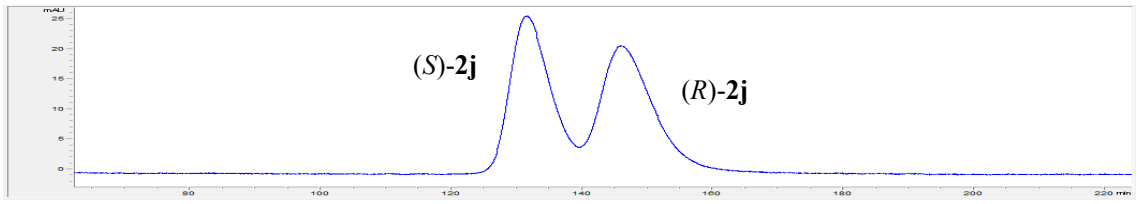
(S)-2j
(R)-2j

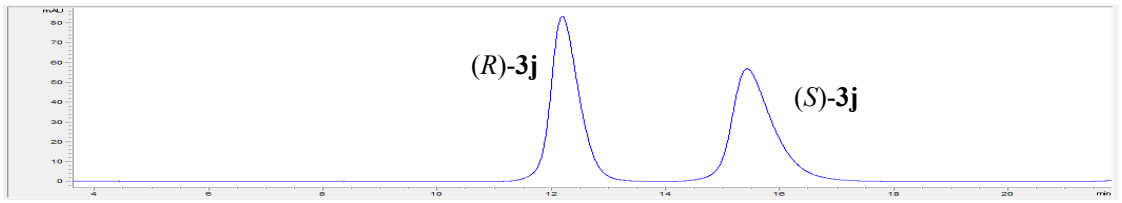
(R)-3j
(S)-3j

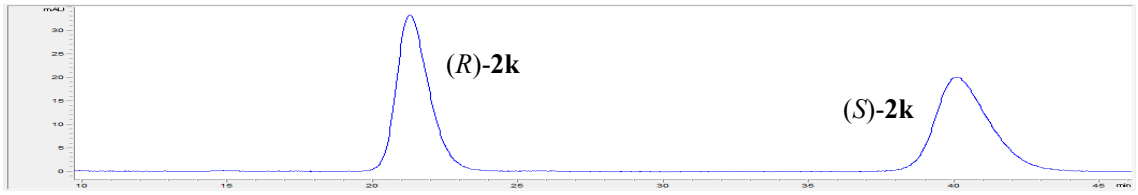
(R)-2k
(S)-2k

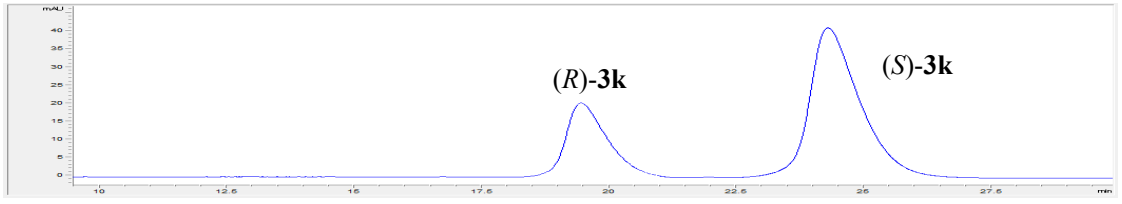
(R)-3k
(S)-3k

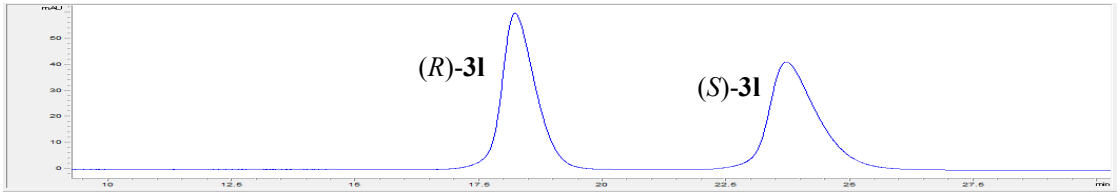
(R)-3l
(S)-3l

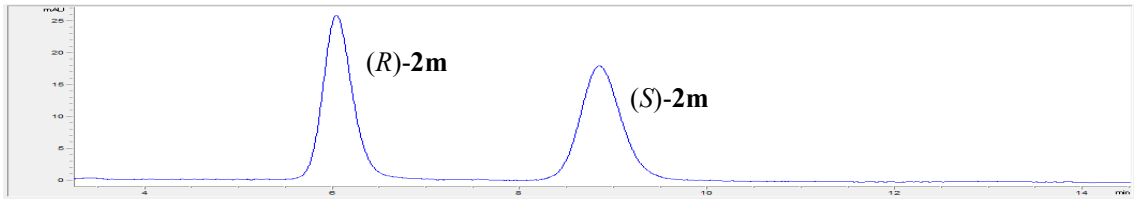
(R)-2m
(S)-2m

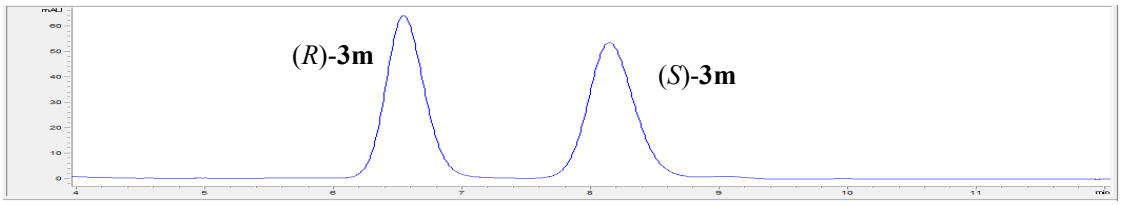
(R)-3m
(S)-3m

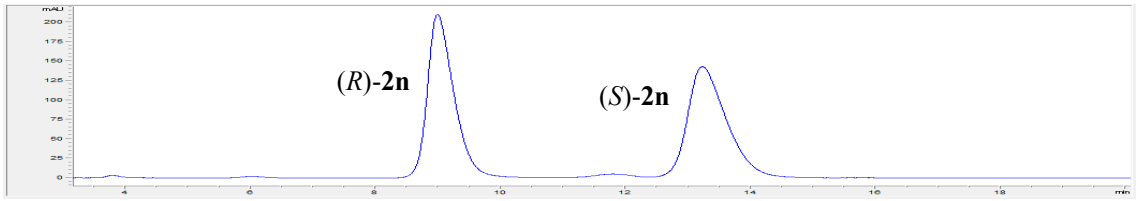
(R)-2n
(S)-2n

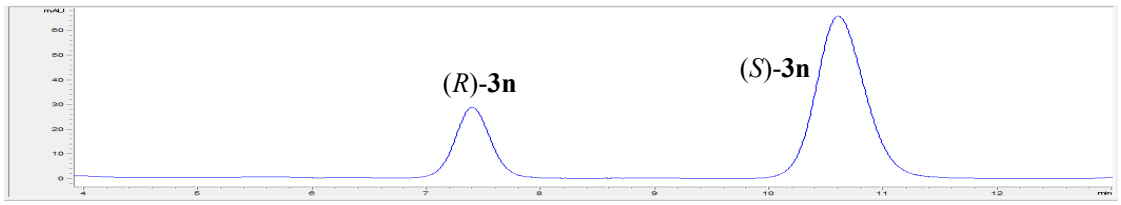
(R)-3n
(S)-3n

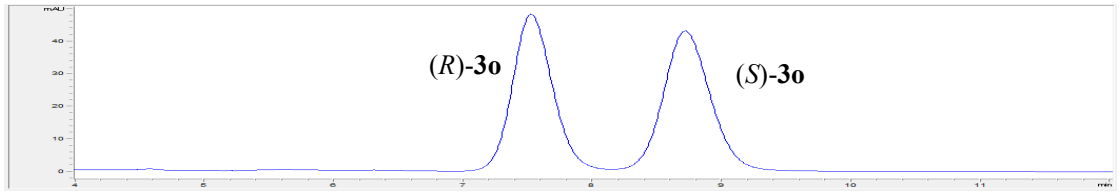
(R)-3o
(S)-3o

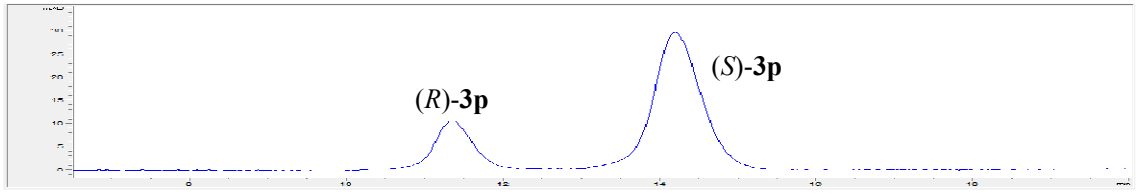
(R)-3p
(S)-3p

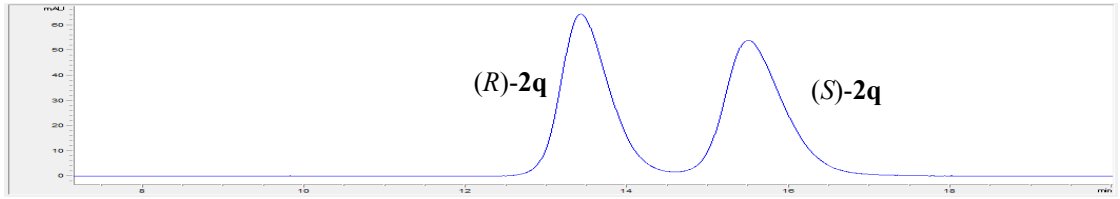
(R)-2q
(S)-2q

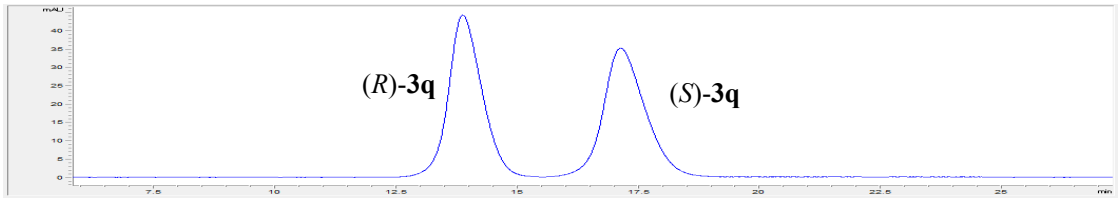
(R)-3q
(S)-3q

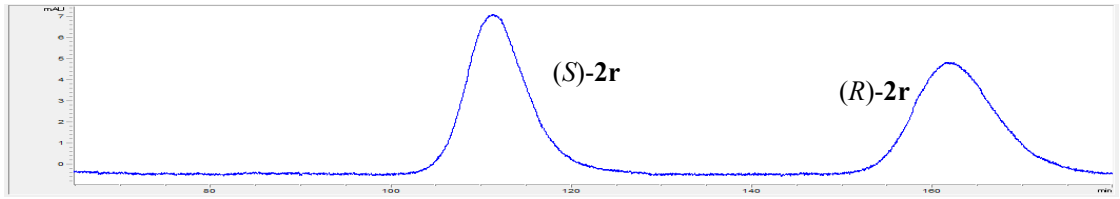
(S)-2r
(R)-2r

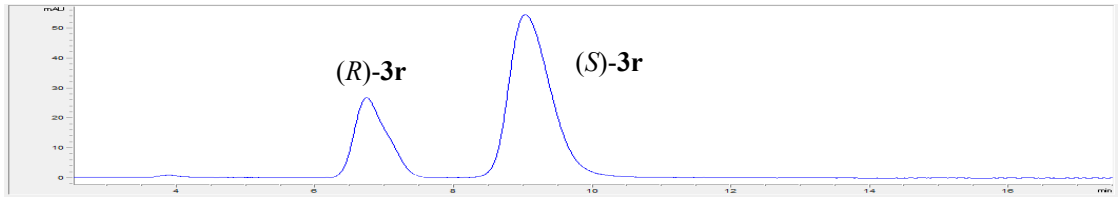
(R)-3r
(S)-3r

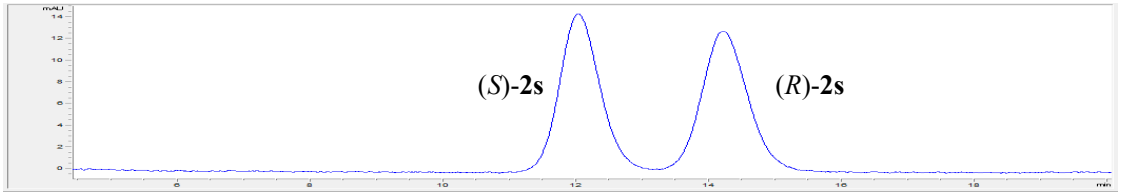
(S)-2s
(R)-2s

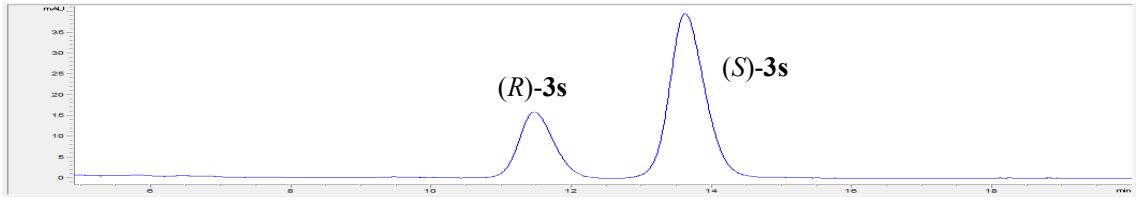
(R)-3s
(S)-3s

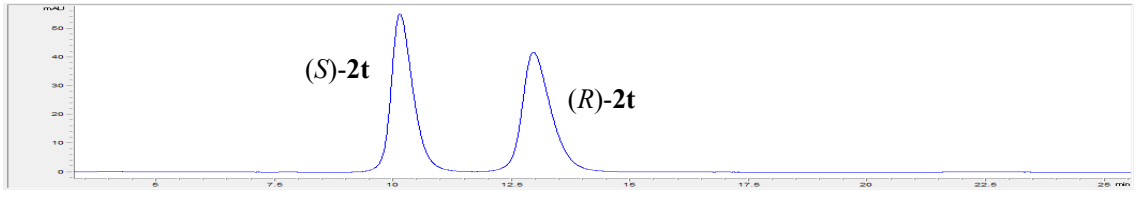
(S)-2t
(R)-2t

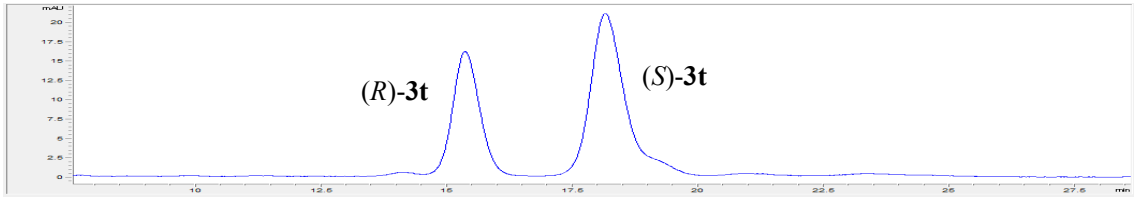
(R)-3t
(S)-3t

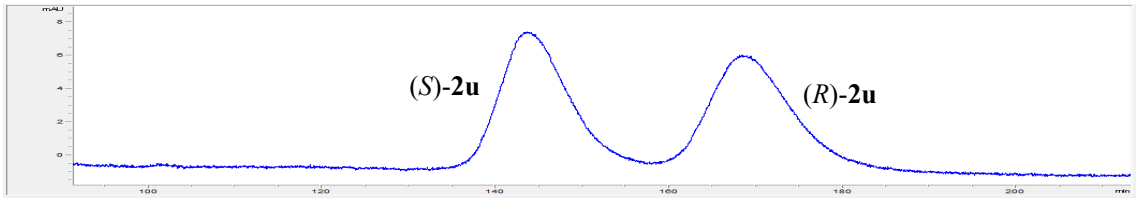
(S)-2u
(R)-2u

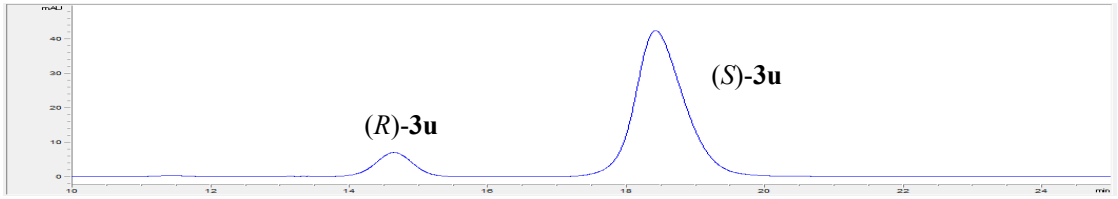
(R)-3u
(S)-3u

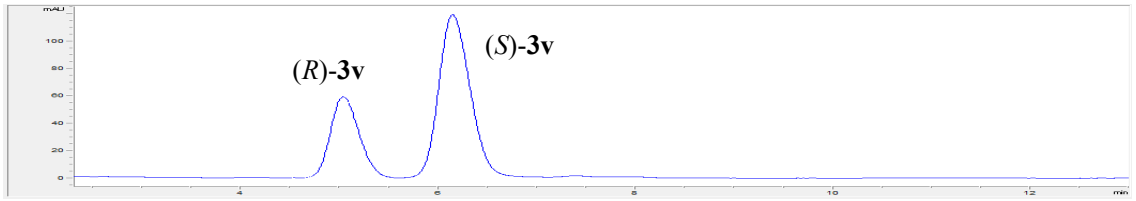
(R)-3v
(S)-3v

Only for compounds **2-3a**, **2-3d** and **2-3r** the low-temperature method employed for the separation of the β-amino acid enantiomers also afforded separation of the α-enantiomers with little or no overlap, as shown by the traces below.

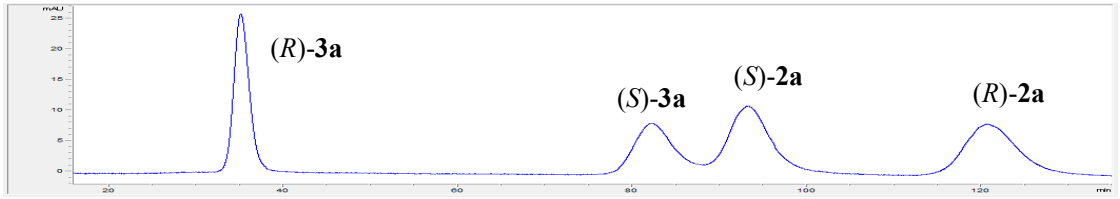

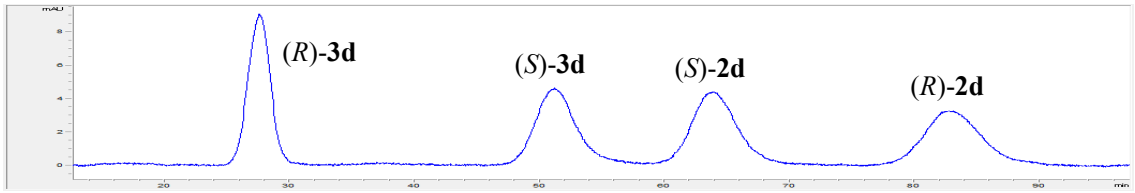

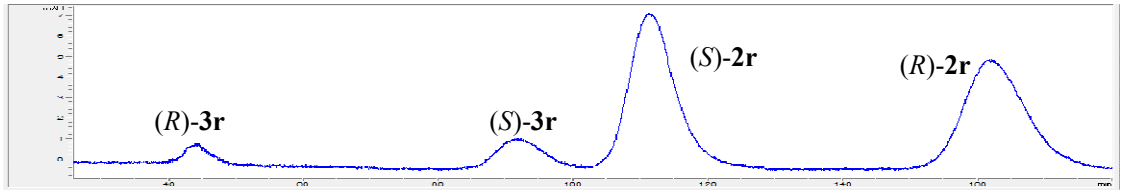

Additional time course experiments

Table S11. Time course of the amination of methylcinnamates **1t-u** to methyl-β-phenylalanines **2t-u** by the EncP-R299K variant.

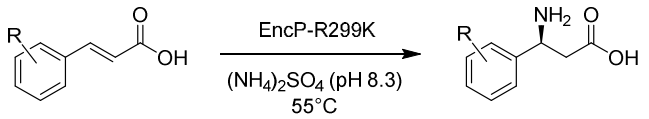

1t, R: 3-Me
1u, R: 4-Me

(*S*)-**2t**, R: 3-Me
(*S*)-**2u**, R: 4-Me

Time (h)	Substrate **1t**			Substrate **1u**		
	Conv. (%)[a]	β:α ratio[a]	ee of **2t** (%)[b]	Conv. (%)[a]	β:α ratio[a]	ee of **2u** (%)[b]
1	6	99:1	>95 (*S*)	9	99:1	–
2	12	99:1	90 (*S*)	11	99:1	87 (*S*)
4	14	99:1	90 (*S*)	18	99:1	86 (*S*)
8	18	99:1	90 (*S*)	21	99:1	87 (*S*)
22	20	99:1	90 (*S*)	21	99:1	86 (*S*)
48	21	99:1	90 (*S*)	21	99:1	87 (*S*)

[a] conversions and product ratios determined by non-chiral HPLC; [b] enantiomeric excesses determined by chiral HPLC.

References

S1. Röther, D.; Poppe, L.; Viergutz, S.; Langer, B.; Rétey, J. Characterization of the active site of histidine ammonia-lyase from *Pseudomonas putida*. *Eur. J. Biochem.* **2001**, *268*, 6011-6019.

S2. Bartsch, S.; Bornscheuer, U. T. Mutational analysis of phenylalanine ammonia lyase to improve reactions rates for various substrates. *Protein Eng. Des. Sel.* **2010**, *23*, 929-933.

S3. Szymanski, W. et al. Phenylalanine aminomutase-catalyzed addition of ammonia to substituted cinnamic acids: a route to enantiopure alpha- and beta-amino acids. *J. Org. Chem.* **2009**, *74*, 9152-9157.

S4. (a) Tan, C. Y. K.; Weaver, D. F. A one-pot synthesis of 3-amino-3-arylpropionic acids. *Tetrahedron* **2001**, *58*, 7449-7461; (b) Busca, P.; Paradisi, F.; Moynihan, E.; Maguire, A. R.; Engel, P. C. Enantioselective synthesis of non-natural amino acids using phenylalanine dehydrogenases modified by site-directed mutagenesis. *Org. Biomol. Chem.* **2004**, *2*, 2684-2691; (c) Bea, H.-S.; Park, H.-J.; Lee, S.-H.; Yun, H. Kinetic resolution of aromatic β-amino acids by ω-transaminase. *Chem. Commun.* **2011**, *47*, 5894-5896.

S5. Parmeggiani, F.; Lovelock, S. L.; Weise, N. J.; Ahmed, S. T.; Turner, N. J. Synthesis of D- and L-phenylalanine derivatives by phenylalanine ammonia lyases: a multienzymatic cascade process. *Angew. Chem. Int. Ed.* **2015**, *54*, 4608-4611.